Cell Reports, Volume *29*

Supplemental Information

A Central Amygdala Input to the Parafascicular Nucleus Controls Comorbid Pain in Depression

Xia Zhu, Wenjie Zhou, Yan Jin, Haodi Tang, Peng Cao, Yu Mao, Wen Xie, Xulai Zhang, Fei Zhao, Min-Hua Luo, Haitao Wang, Jie Li, Wenjuan Tao, Zahra Farzinpour, Likui Wang, Xiangyao Li, Juan Li, Zheng-Quan Tang, Chenghua Zhou, Zhizhong Z. Pan, and Zhi Zhang

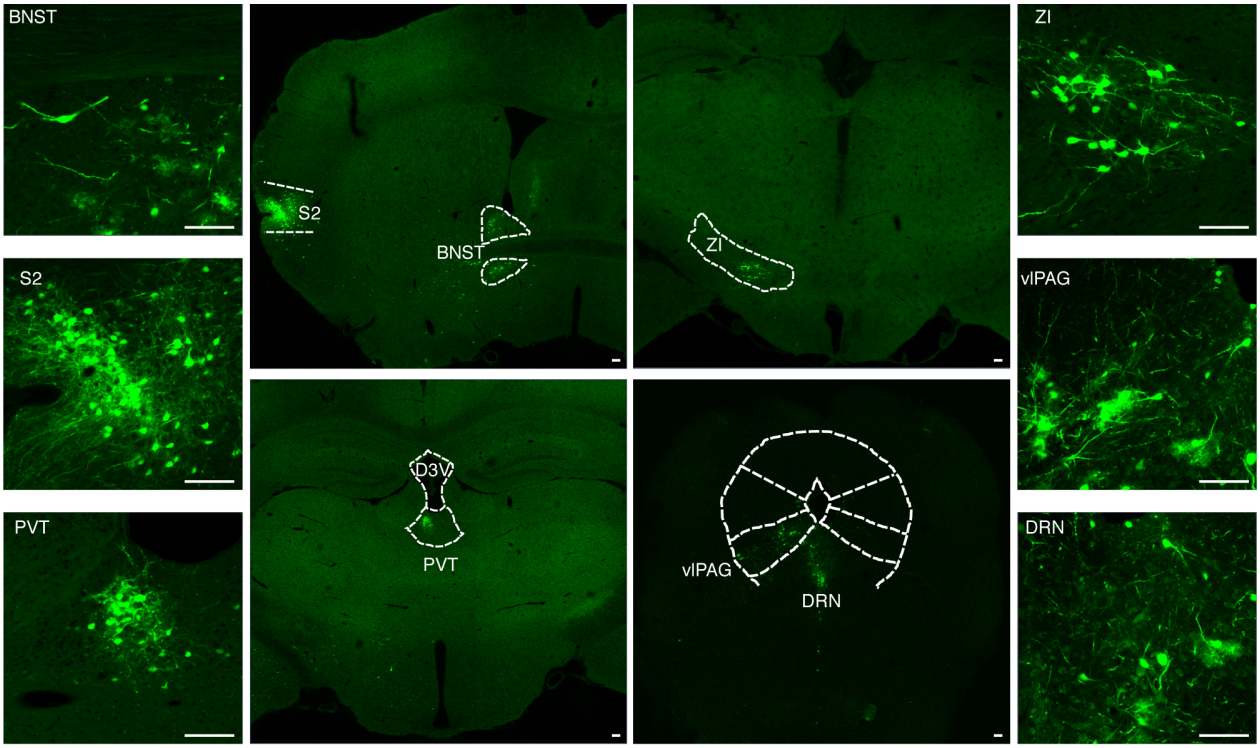

Figure S1. Mapping outputs of CeA neurons. Related to Figure 1.

Images representation of GFP labeling neurons by CeA infusion of H129-GFP4. BNST, bed nucleus of the stria terminalis; S2, secondary somatosensory cortex; PVT, paraventricular nucleus of the thalamus; ZI, zona incerta; vlPAG, ventrolateral periaqueductal gray; DRN, dorsal raphe nucleus; D3V, dorsal 3rd ventricle; Aq, aqueduct. Scale bar, 200 μm.

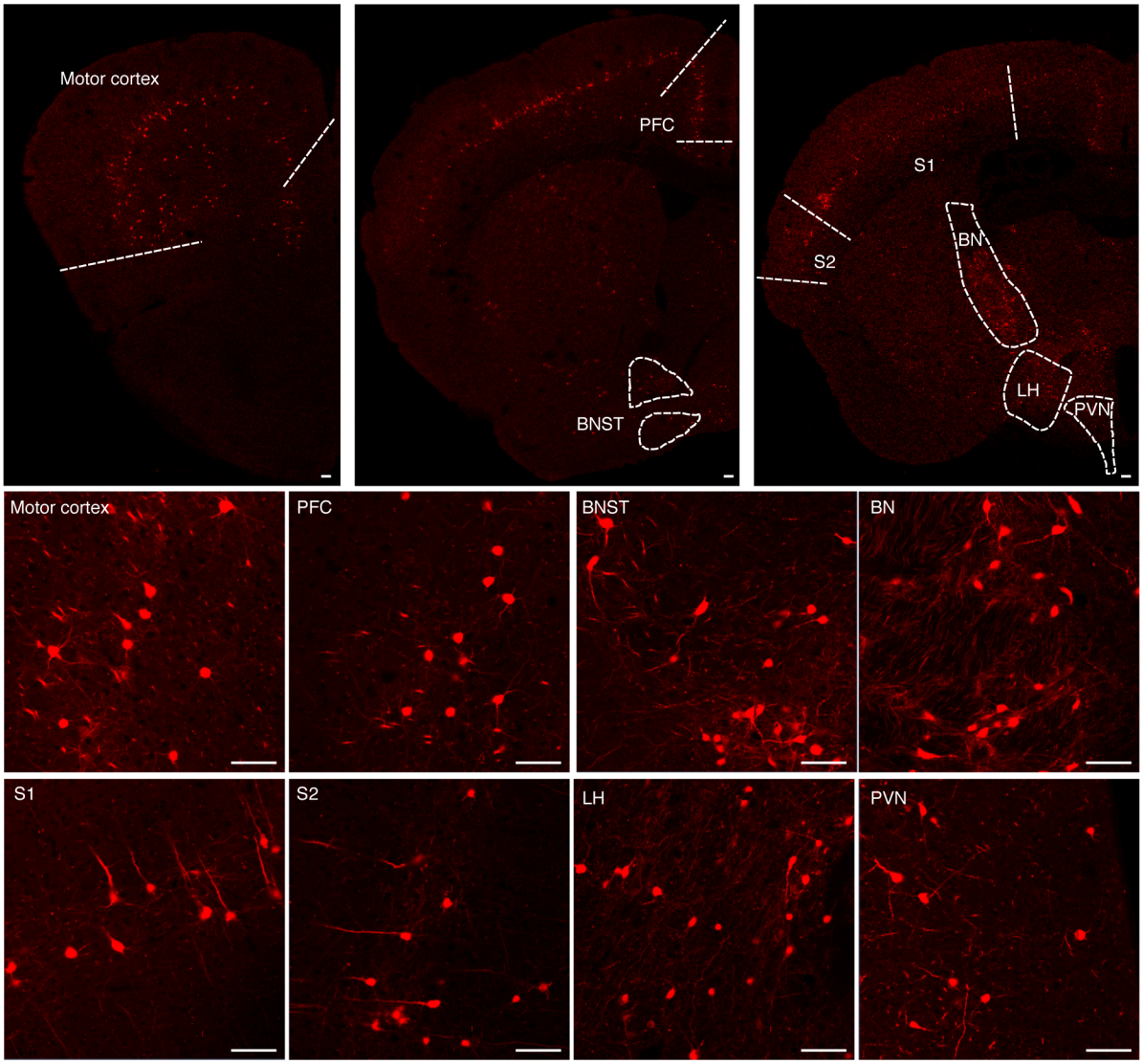

Figure S2. Mapping inputs of Glu^{PF} neurons and GABA^{PF} neurons. Related to Figure 1.
Coronal images representation of Cre-dependent retrograde trans-monosynaptic rabies virus tracing strategy in the PF of *CaMKII-Cre* mice, [as shown in (Figure 1D)]. DsRed-labeled neurons were detected within multiple brain regions. M1 and M2, primary motor cortex; PFC, prefrontal cortex; BNST, bed nucleus of the stria terminalis; BN, basal nucleus; S1, primary somatosensory cortex; S2, secondary somatosensory cortex; LH, lateral hypothalamus; PVN, paraventricular thalamic nucleus. Scale bar, 200 μm.

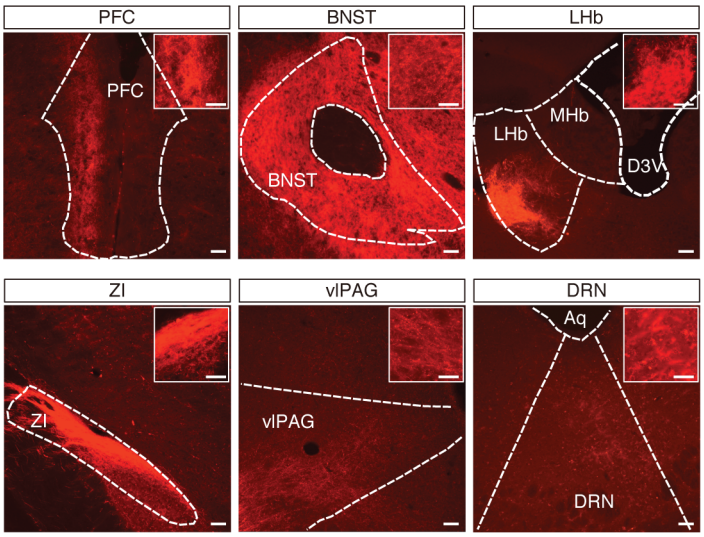

Figure S3. Mapping outputs of GABA^{CeA} neurons. Related to Figure 2.

Images represent mCherry^{+} fibers in *GAD2-Cre* mice with CeA injection of AAV-DIO-ChR2-mCherry. PFC, prefrontal cortex; BNST, bed nucleus of the stria terminalis; MHb, medial habenular nucleus; LHb, lateral habenular nucleus; ZI, zona incerta; vlPAG, ventrolateral periaqueductal gray; DRN, dorsal raphe nucleus; D3V, dorsal 3rd ventricle; Aq, aqueduct. Scale bars, 100 μm. The white boxes depicting the area shown interested regions. Scale bars, 20 μm.

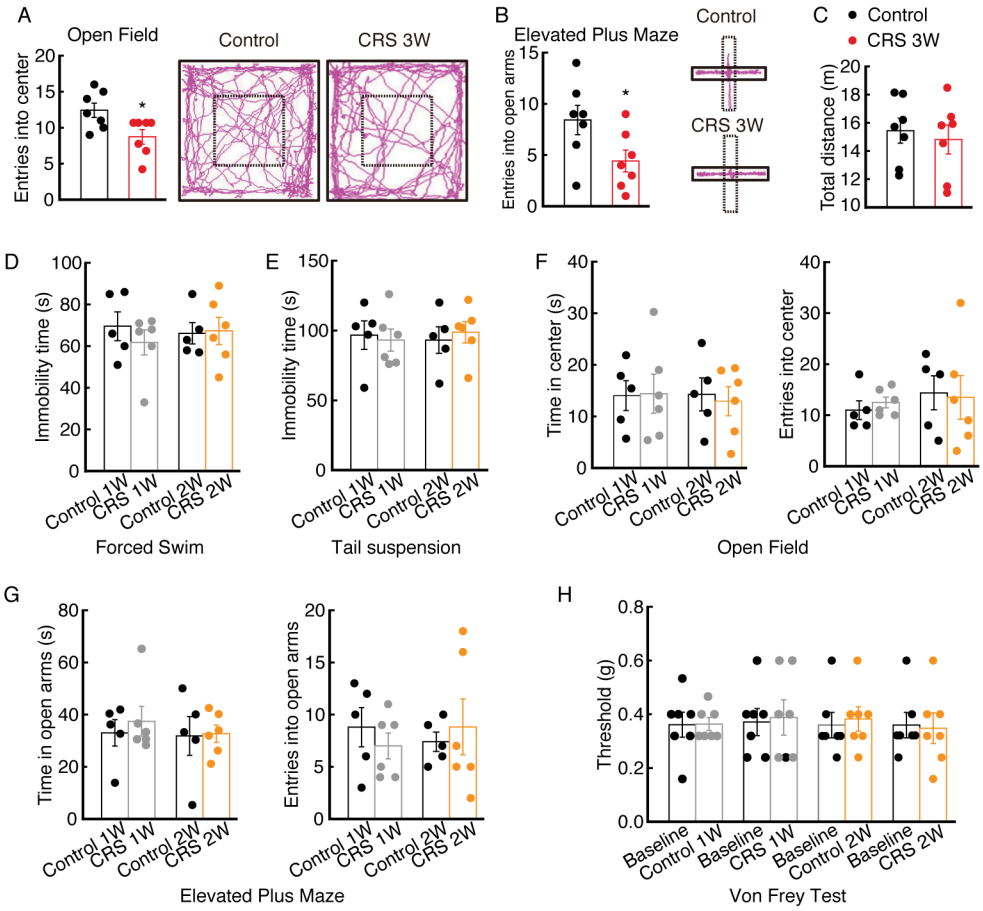

Figure S4. CRS 1W or CRS 2W mice did not display pain sensitization and depressive-like behaviors. Related to Figure 3.

(A-C) Entries into the center of the open field (A) and the open arms of the elevated plus maze (B) decreased in CRS 3W mice when compared to control mice. The total distance in the open field was not changed (C). Traces in the (A) and (B) represent animal movement path. (n = 7 mice per group.)

(D-H) No behavioral difference was observed for CRS 1W or 2W mice in forced swim (D), tail suspension (E), open field test (F), elevated plus maze (G), and Von Frey (H) when compared to control mice (n = 5-6 mice). All data are presented as mean ± SEM. * $P < 0.05$. Unpaired t test for (A), (B) and (C); Paired t test for (H); One-way ANOVA with Bonferroni post hoc analysis for (D), (E), (F), and (G).

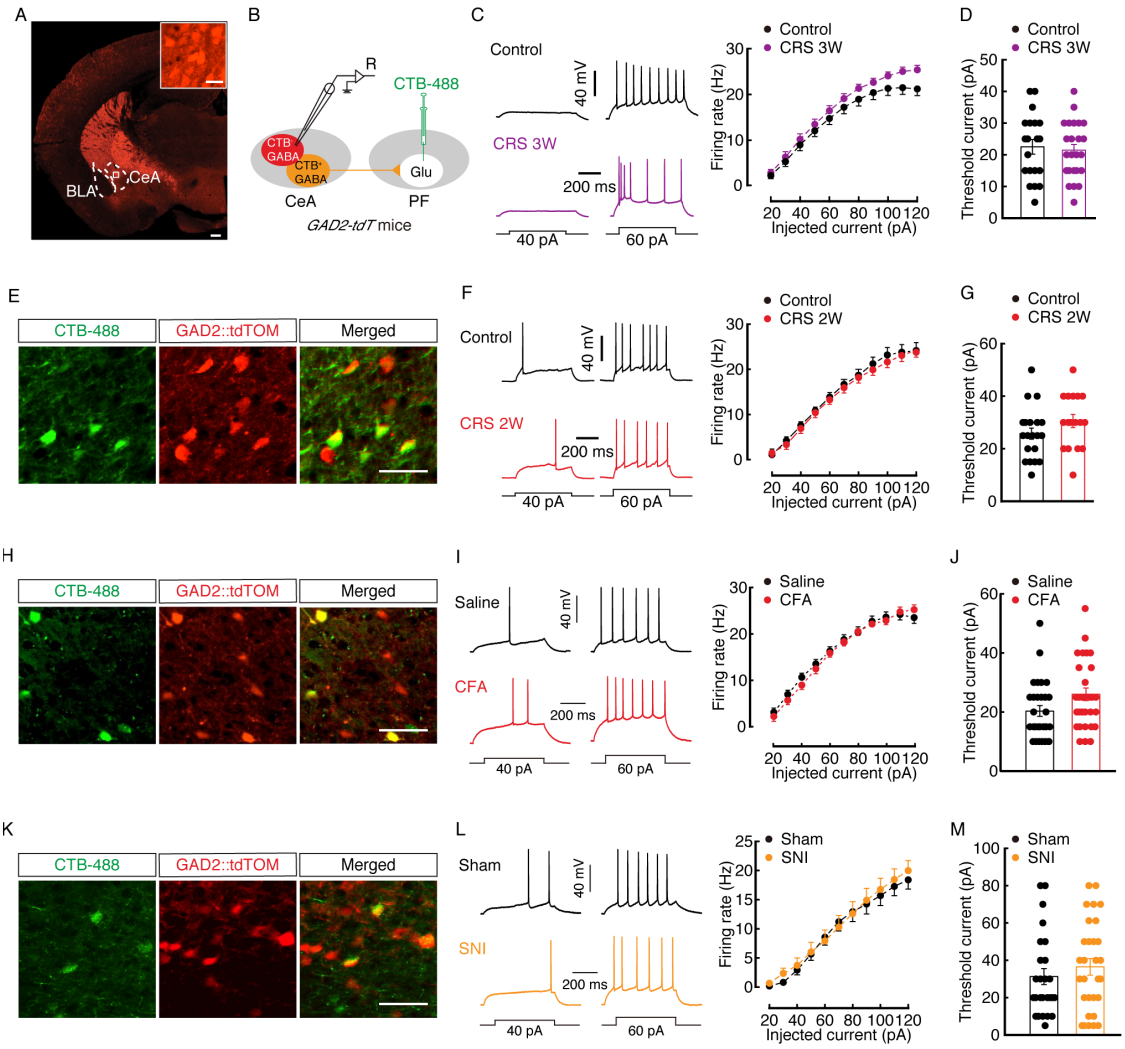

Figure S5. CRS 2W, CFA 3D or SNI 7D had no effect on PF-projecting GABA^{CeA} neuronal activity. Related to Figure 4.

(A) Typical images of GABA neurons expressing tdTomato (red) in *GAD2-tdT* mice (scale bar, 200 μm).

The box depicting the area shown in the CeA (scale bar, 20 μm).

(B) Schematic of CTB^{-}488 injection and recording configuration in acute slices.

(C and D) Sample traces and statistical data for firing rate (C) and rheobase (D) recorded from CTB^{-} GABA^{CeA} neurons (red cells in B) in mice treated with control (n = 20 neurons) or CRS 3W (n = 24 neurons).

(E) Representative images of GABA^{CeA} neurons (yellow) labeled by CTB-488 (green) injected in the CeA of *GAD2-tdTOM* mice (neurons with red tdTOM). Scale bar, 50 μm.

(F and G) Action potential firing rate (F) and rheobase (G) recorded from GABA^{CeA} neurons in mice treated with control (n = 17 neurons) and CRS 2W (n = 20 neurons).

(H) Representative images of GABA^{CeA} neurons (yellow) labeled by CTB-488 (green) injected in the CeA of *GAD2-tdTOM* mice (neurons with red tdTOM). Scale bar, 50 μm.

(I and J) Action potential firing rate (I) and rheobase (J) recorded from $GABA^{CeA}$ neurons in mice treated with saline (n = 29 neurons) and CFA 3D (n = 30 neurons).
(K) Representative images of $GABA^{CeA}$ neurons (yellow) labeled by CTB-488 (green) injected in the CeA of *GAD2-tdTOM* mice (neurons with red tdTOM). Scale bar, 50 μm.
(L and M) Action potential firing rate (L) and rheobase (M) recorded from $GABA^{CeA}$ neurons in mice treated with sham (n = 30 neurons) and SNI 7D (n = 26 neurons). All data are presented as mean ± SEM. Unpaired t test for (D), (G), (J) and (M); Two-way repeated measures ANOVA with Bonferroni post hoc analysis for (C), (F), (I), and (L).

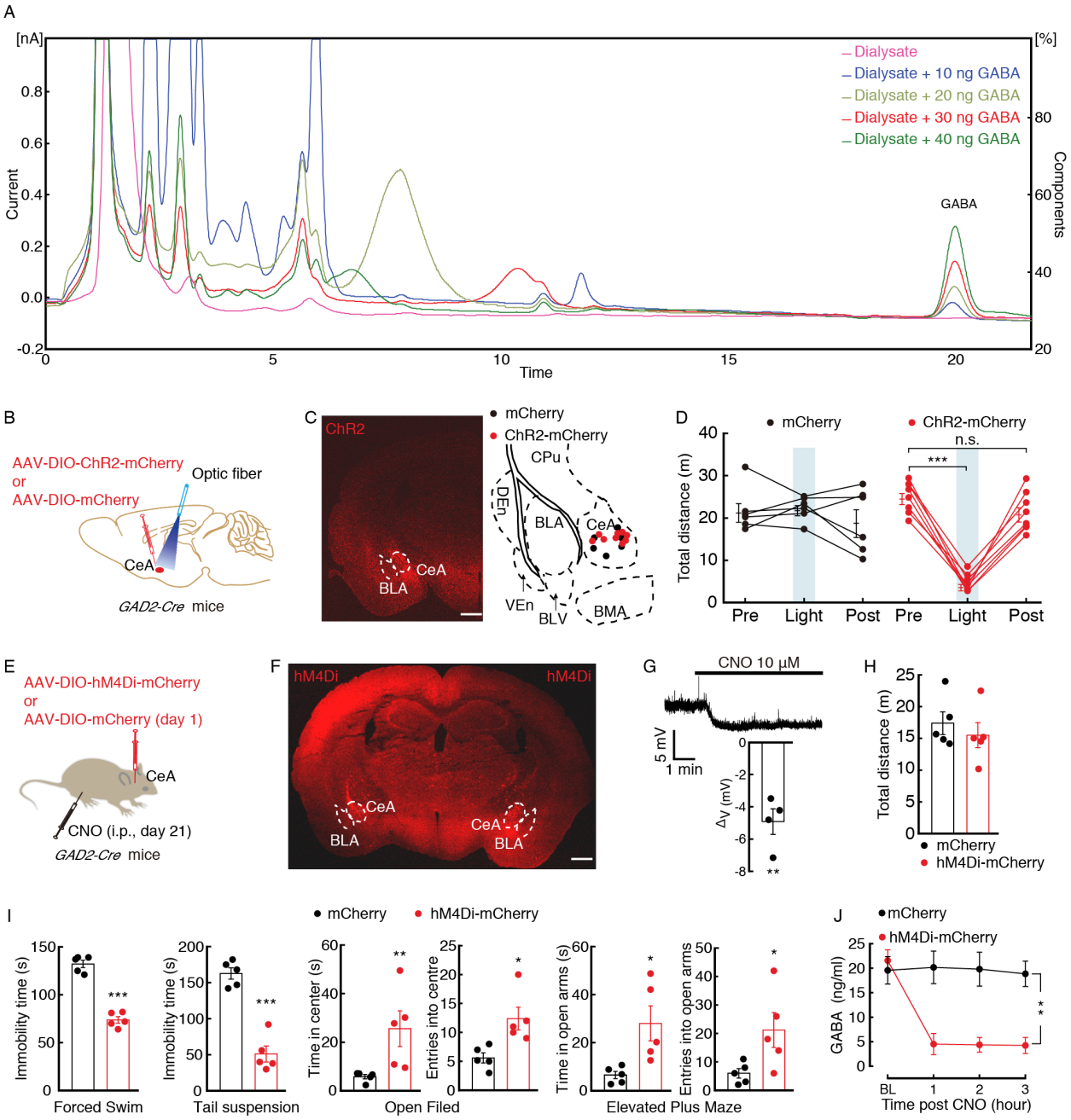

Figure S6. Enhanced inhibition of the GABA^{CeA}→ Glu^{PF} pathway in CP. Related to Figure 4 and STAR Methods.

(A) The standard curve of GABA concentrations in HPLC chromatograms.

(B) Schematic of optogenetics in *GAD2-Cre* mice.

(C) Typical image (left) and injection site (right) with AAV-DIO-ChR2-mCherry of CeA in *GAD2-Cre* mice, Scale bars, 200 μm.

(D) Locomotion in the open filed test before, with and after light photostimulation in mCherry (n = 6) or ChR2-mCherry mice (n = 8).

(E) Schematic of chemogenetics in *GAD2-Cre* mice.

(F) Typical image with AAV-DIO-hM4Di-mCherry of CeA in *GAD2-Cre* mice, Scale bars, 200 μm.
(G) Sample trace (upper) and summary data (lower) from acute slices by whole-cell recording showing hyperpolarization of $GABA^{CeA}$ neurons expressing AAV-DIO-hM4Di-mCherry following bath application of CNO (n = 4 cells from 3 mice).
(H) The total distance of the open field was not changed in the mCherry (n = 5) or hM4Di-mCherry mice (n = 5).
(I) Behavioral effects of chemogenetic inhibition of $GABA^{CeA}$ neurons at 30 min after CNO intraperitoneal injection (i.p., n = 5 mice per group).
(J) Time course of GABA signal in the PF before and after CNO injection (n = 5 mice per group). All data are presented as mean ± SEM. * $P < 0.05$, ** $P < 0.01$, *** $P < 0.001$. One-sample t test for (G); Unpaired t test for (H) and (I); Two-way repeated measures ANOVA with Bonferroni post hoc analysis for (D) and (J).

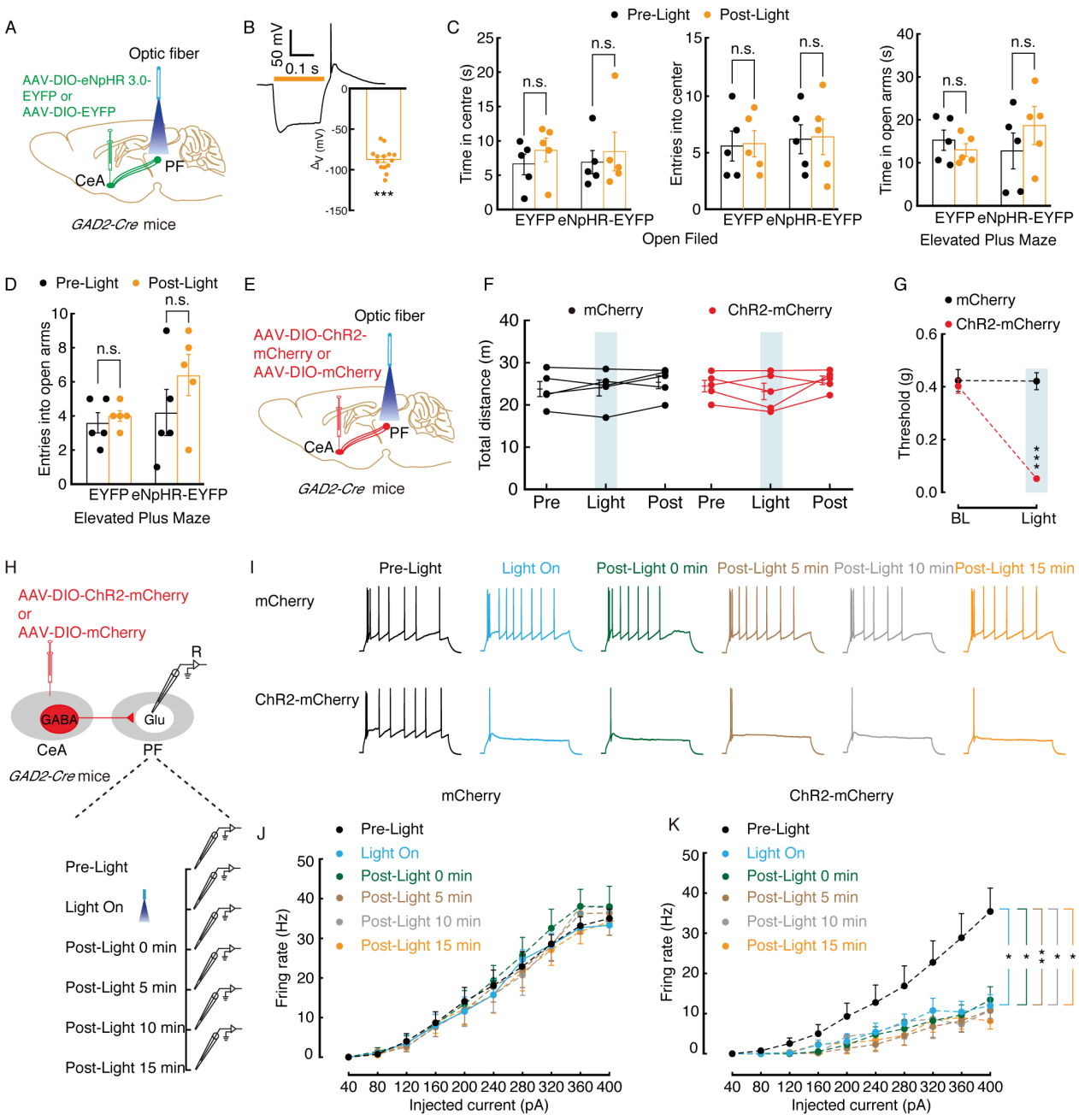

Figure S7. Necessary and sufficient role of the GABA^{CeA}→ Glu^{PF} pathway for CP. Related to Figure 5.

(A) Schematic of optogenetic experiments in *GAD2-Cre* mice.

(B) Sample trace (upper) and statistical data (lower) of currents recorded from AAV-DIO-eNpHR3.0-EYFP-expressing Glu^{PF} neurons via photostimulation (594 nm) in acute slices from *GAD2-Cre* mice (n = 14 neurons).

(C and D) CRS 3W mice with CeA infusion of eNpHR3.0-EYFP or EYFP in testing of open field and elevated plus maze.

(E) Schematic of optogenetic experiments in *GAD2-Cre* mice.

(F) Locomotion in the open filed test before, with and after light photostimulation in mCherry (n = 5) or ChR2-mCherry mice (n = 5).
(G) Effects of optogenetic activation of $GABA^{CeA}$ terminals in the PF on pain threshold in naïve mice (n = 5 mice per group).
(H) Schematic of CeA injection of AAV-DIO-ChR2-mCherry or AAV-DIO-mCherry in *GAD2-Cre* mice and recording configuration in acute slices.
(I-K) Sample traces (I) and summarized data (J and K) of action potentials evoked by 473 nm light recorded from CeA $mCherry^+$ neurons in acute brain slices. All data are presented as mean ± SEM. * $P < 0.05$, ** $P < 0.01$, *** $P < 0.001$. One-sample t test for (B); Paired t test for (C) and (D); Two-way repeated measures ANOVA with Bonferroni post hoc analysis for (F), (G), (J) and (K).

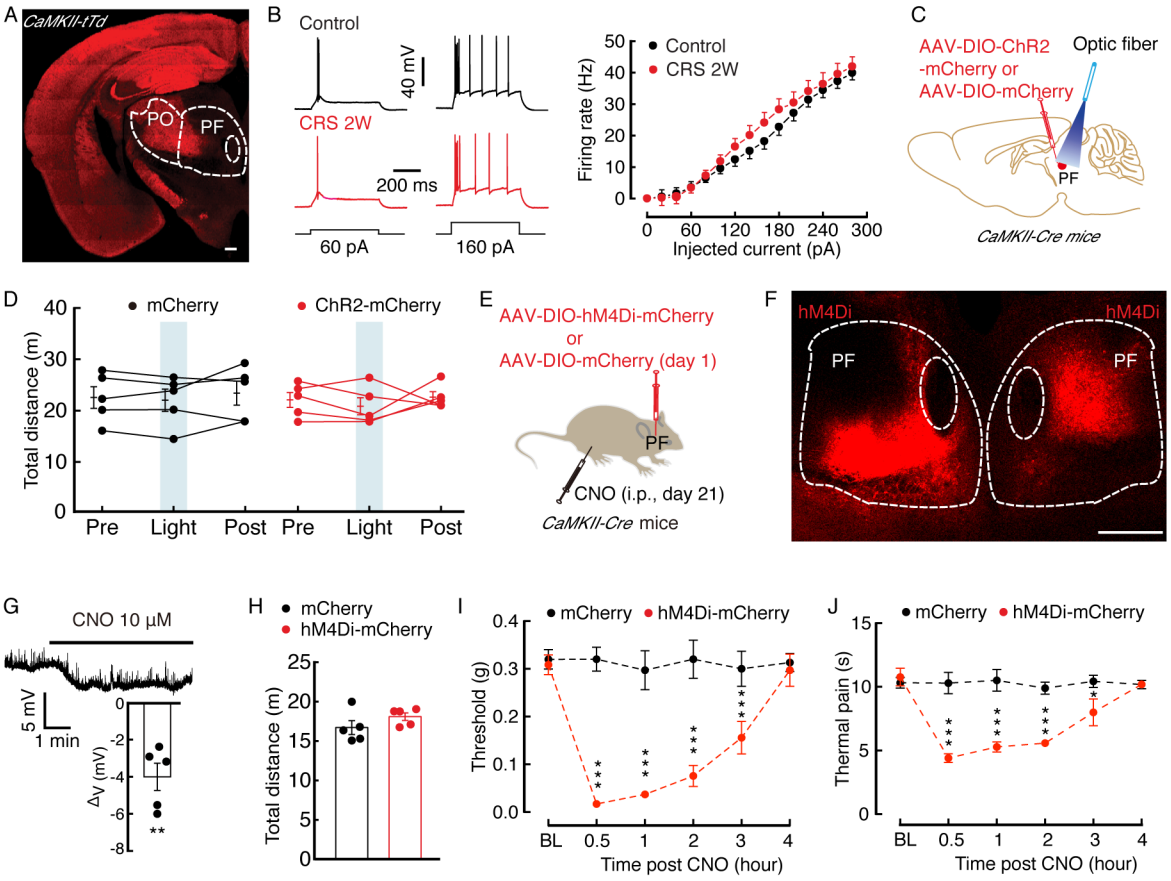

Figure S8. The Glu^{PF} neuronal excitability were not change in CRS 2W mice. Related to Figure 5.

(A) Image showed Glu^{PF} neurons expressing tdTomato in *CaMKII-tdT* mice, which were spliced with a confocal microscope. Scale bar, 200 μm.

(B) Action potential firing rate from Glu^{PF} neurons of CRS 2W mice (n = 21 neurons) and control mice (n = 20 neurons).

(C) Schematic of optogenetic experiments in *CaMKII-Cre* mice.

(D) Locomotion in the open filed test before, with and after light photostimulation in mCherry (n = 5) or ChR2-mCherry mice (n = 5).

(E) Schematic of chemogenetics in *CaMKII-Cre* mice.

(F) Typical image with AAV-DIO-hM4Di-mCherry of PF in *CaMKII-Cre* mice, Scale bars, 200 μm.

(G) Sample trace (upper) and summary data (lower) from acute slices by whole-cell recording showing hyperpolarization of Glu^{PF} neurons expressing AAV-DIO-hM4Di-mCherry following bath application of CNO (n = 5 cells from 3 mice).

(H) The total distance of the open field was not changed in the mCherry (n = 5) or hM4Di-mCherry mice (n = 5).

(I and J) Behavioral effects of chemogenetic inhibition of GABA^{CeA} neurons on mechanical (I) and thermal (J) pain threshold in *CaMKII-Cre* naïve mice (n = 5 mice per group). All data are presented as mean ± SEM. * $P < 0.05$, ** $P < 0.01$, *** $P < 0.001$. One-sample t test for (G); Unpaired t test for (H); Two-way repeated measures ANOVA with Bonferroni post hoc analysis for (B), (D), (I) and (J).

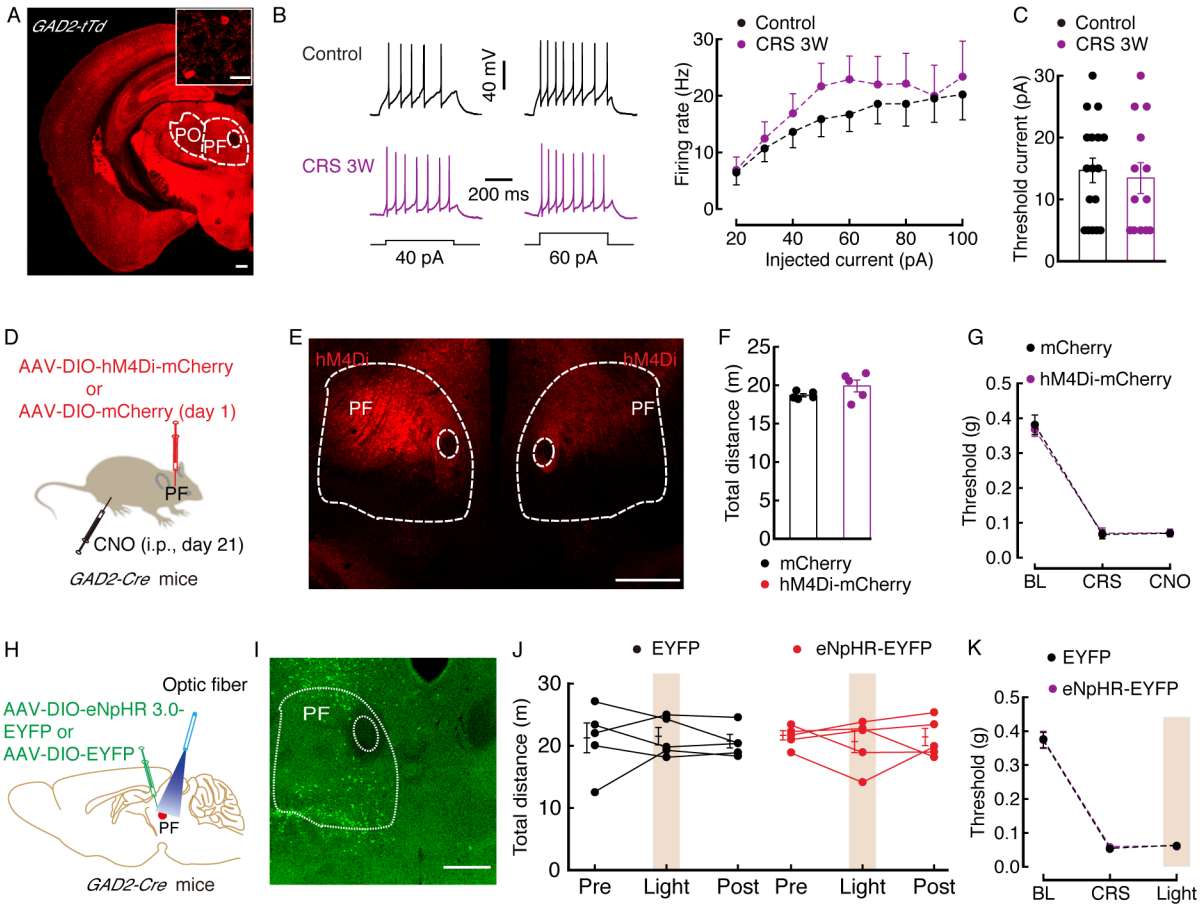

Figure S9. GABA^{PF} neuronal excitability was not changed in CRS 3W mice. Related to Figure 5.

(A) Typical images of GABA neurons expressing tdTomato (red) in *GAD2-tdT* mice (scale bar, 200 μm). The box depicting the area shown in the PF (scale bar, 20 mm).

(B and C) Action potential firing rate (B) and rheobase (C) recorded from GABA^{PF} neurons in control mice (n = 17 neurons) and CRS 3W mice (n = 13 neurons).

(D) Schematic of chemogenetics in *GAD2-Cre* mice.

(E) Typical image with AAV-DIO-hM4Di-mCherry of PF in *GAD2-Cre* mice, Scale bars, 200 μm.

(F) The total distance of the open field was not changed in the mCherry (n = 5) or hM4Di-mCherry mice (n= 5).

(G) Behavioral effects of chemogenetic inhibition of GABA^{PF} neurons on pain threshold in *GAD2-Cre* mice CRS 3W mice (n = 5 mice per group).

(H) Schematic of chemogenetics in *GAD2-Cre* mice.

(I) Typical image with AAV-DIO-eNpHR-EYFP of PF in *GAD2-Cre* mice, Scale bars, 200 μm.

(J) Locomotion in the open filed test before, with and after light photostimulation in EYFP (n = 5) or eNpHR-EYFP mice (n = 5).

(K) Effects of optogenetic activation of GABA^{PF} neurons on pain threshold in *GAD2-Cre* mice CRS 3W mice (n = 5 mice per group). All of the data are presented as mean ± SEM. Unpaired t test for (C) and (F); Two-way repeated measures ANOVA with Bonferroni post hoc analysis for (B), (G), (J) and (K).

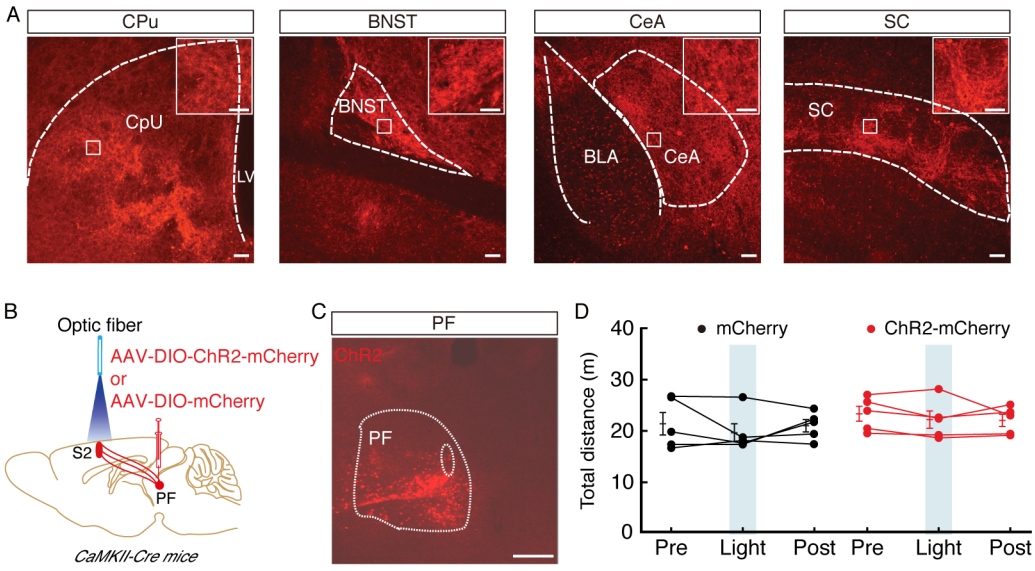

Figure S10. Mapping outputs of Glu^{PF} neurons. Related to Figure 6.

(A) Representative image of mCherry signals at day 21 after PF infusion of AAV-DIO-ChR2-mCherry in *CaMKII-Cre* mice. CPu, caudate putamen; BNST, Bed Nucleus of the Stria Terminalis; CeA, central amygdaloid nucleus; SC, superior colliculus; LV, lateral ventricle; BLA, basolateral amygdaloid nucleus. Scale bar, 100 μm. The white boxes depicting the area shown interested regions. Scale bar, 20 μm.

(B) Schematic of optogenetic in *CaMKII-Cre* mice.

(C) Typical image with AAV-DIO-ChR2-mCherry of PF in *CaMKII-Cre* mice, Scale bars, 200 μm.

(D) Locomotion in the open filed test before, with and after light photostimulation in mCherry (n = 5) or ChR2-mCherry mice (n = 5). All data are presented as mean ± SEM. Two-way repeated measures ANOVA with Bonferroni post hoc analysis for (D).

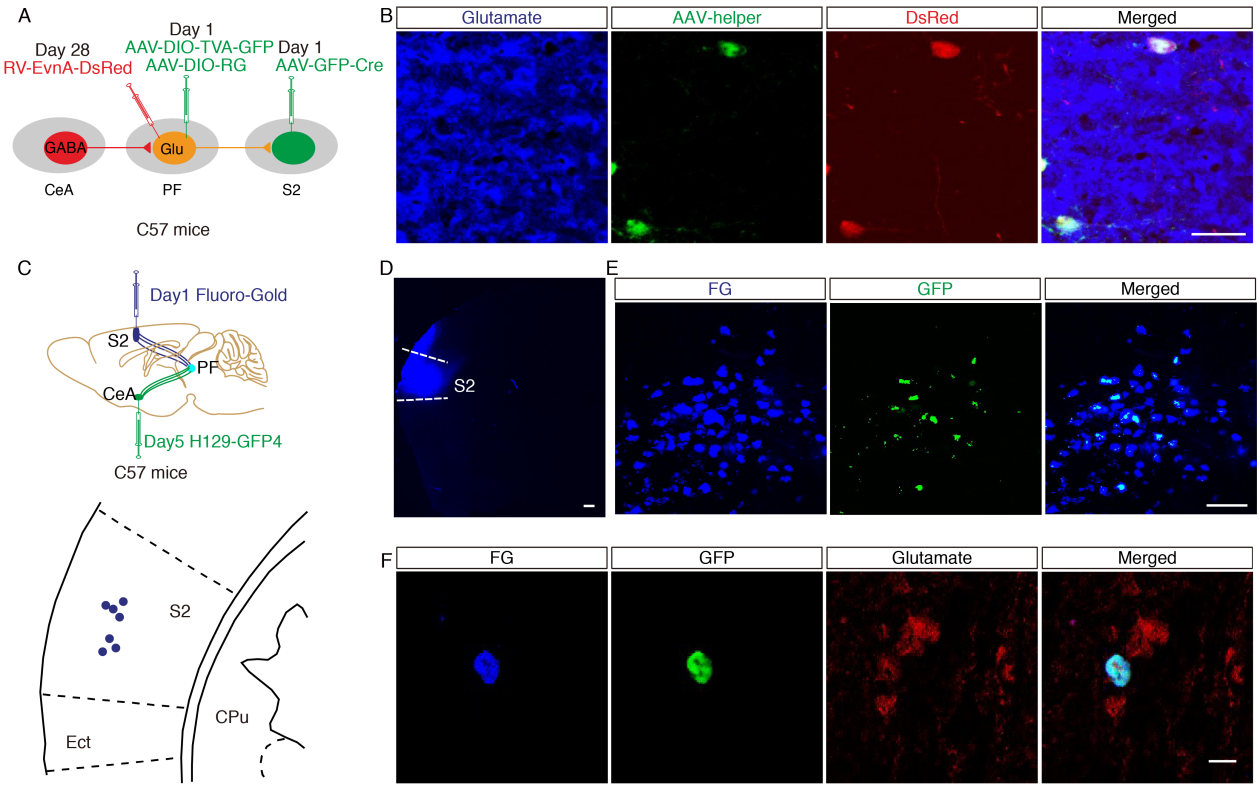

Figure S11. Dissection of the GABA^{CeA}→Glu^{PF}→S2 pathway. Related to Figure 7.

(A) Schematic of viral injection for triple retrograde tracing.

(B) AAV-GFP-Cre-infected PF neurons, which project to the CeA as indicated in Figure 7B middle, are glutamate neurons based on immunofluorescence staining. Representative images of glutamate neurons (blue), AAV-helper (green), DsRed (red), and merged (white) glutamate neurons in the PF. Scale bar, 100 μm.

(C) Tracing scheme (upper) and injection site of S2 (lower) for CeA-PF-S2 pathway combing with Fluoro-Gold and H129-G4.

(D) Representative image of Fluoro-Gold signals in the S2 in C57 mice. Scale bars, 200 μm.

(E and F) Representative images of PF neurons infected with H129-G4 (green) and FG (blue; E, Scale bar, 20 μm), which are colocalized with glutamate immunofluorescence (F, Scale bar, 20 μm).

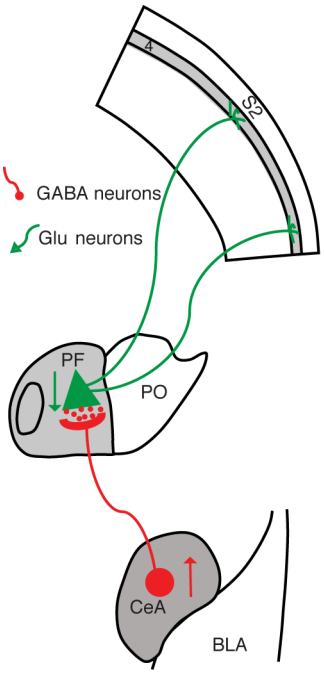

Figure S12. A model of enhanced inhibitory GABA^{CeA}→Glu^{PF}→S2 pathway in CP. Related to Figure 7.

In the depression state, an enhanced inhibitory process occurs within the PF, which involves increased GABA^{CeA} inputs that mediate inhibition of the Glu^{PF} (green). The alterations lead to low excitation of the Glu^{PF} neurons. As a result, the Glu^{PF} excitatory outputs (yellow) to the S2 are decreased, and presumably causes CP symptoms. CeA, central nucleus of the amygdala; PF, parafascicular nucleus; S2, second somatosensory cortex; Glu, glutamate; GABA, gamma-aminobutyric acid.